RESEARCH ARTICLE
Molecular Biology and Physiology

# High-Resolution Genome-Wide Occupancy in *Candida* spp. Using ChEC-seq

**Faiza Tebbji,[a] Inès Khemiri,[a,b] Adnane Sellam[a,b]**

[a]Montreal Heart Institute, Université de Montréal, Montréal, Quebec, Canada
[b]Department of Microbiology, Infectious Diseases and Immunology, Faculty of Medicine, Université de Montréal, Montréal, Quebec, Canada

**ABSTRACT** To persist in their dynamic human host environments, fungal pathogens must sense and adapt by modulating their gene expression to fulfill their cellular needs. Understanding transcriptional regulation on a global scale would uncover cellular processes linked to persistence and virulence mechanisms that could be targeted for antifungal therapeutics. Infections associated with the yeast *Candida albicans*, a highly prevalent fungal pathogen, and the multiresistant related species *Candida auris* are becoming a serious public health threat. To define the set of a gene regulated by a transcriptional regulator in *C. albicans*, chromatin immunoprecipitation (ChIP)-based techniques, including ChIP with microarray technology (ChIP-chip) or ChIP-DNA sequencing (ChIP-seq), have been widely used. Here, we describe a new set of PCR-based micrococcal nuclease (MNase)-tagging plasmids for *C. albicans* and other *Candida* spp. to determine the genome-wide location of any transcriptional regulator of interest using chromatin endogenous cleavage (ChEC) coupled to high-throughput sequencing (ChEC-seq). The ChEC procedure does not require protein-DNA cross-linking or sonication, thus avoiding artifacts related to epitope masking or the hyper-ChIPable euchromatic phenomenon. In a proof-of-concept application of ChEC-seq, we provided a high-resolution binding map of the SWI/SNF chromatin remodeling complex, a master regulator of fungal fitness in *C. albicans*, in addition to the transcription factor Nsi1 that is an ortholog of the DNA-binding protein Reb1 for which genome-wide occupancy was previously established in *Saccharomyces cerevisiae*. The ChEC-seq procedure described here will allow a high-resolution genomic location definition which will enable a better understanding of transcriptional regulatory circuits that govern fungal fitness and drug resistance in these medically important fungi.

**IMPORTANCE** Systemic fungal infections caused by *Candida albicans* and the "superbug" *Candida auris* are becoming a serious public health threat. The ability of these yeasts to cause disease is linked to their faculty to modulate the expression of genes that mediate their escape from the immune surveillance and their persistence in the different unfavorable niches within the host. Comprehensive knowledge on gene expression control of fungal fitness is consequently an interesting framework for the identification of essential infection processes that could be hindered by chemicals as potential therapeutics. Here, we expanded the use of ChEC-seq, a technique that was initially developed in the yeast model *Saccharomyces cerevisiae* to identify genes that are modulated by a transcriptional regulator, in pathogenic yeasts from the genus *Candida*. This robust technique will allow a better characterization of key gene expression regulators and their contribution to virulence and antifungal resistance in these pathogenic yeasts.

**KEYWORDS** *Candida albicans*, *Candida* spp., ChEC-seq, genome-wide occupancy, transcriptional regulatory network

**Citation** Tebbji F, Khemiri I, Sellam A. 2020. High-resolution genome-wide occupancy in *Candida* spp. using ChEC-seq. mSphere 5: e00646-20. https://doi.org/10.1128/mSphere.00646-20.

**Editor** Aaron P. Mitchell, University of Georgia



Address correspondence to Adnane Sellam, adnane.sellam@umontreal.ca.

**Received** 30 June 2020
**Accepted** 28 September 2020
**Published** 14 October 2020

*Candida* species, in particular *Candida albicans*, are major components of the disease burden caused by fungi and are frequent causes of life-threatening invasive infections especially in immunocompromised patients. The emergent *Candida auris* was the first fungal pathogen considered an urgent public health threat due to its multidrug resistance, high transmissibility among patients in health care facilities, and elevated crude mortality (1). Other *Candida* species such as *C. parapsilosis*, *C. tropicalis*, *C. guilliermondii*, and the azole-resistant yeasts *C. glabrata* and *C. krusei* are also frequent causes of candidiasis and vulvovaginal infections (2–4). Current anti-*Candida* therapeutics suffer from diverse limitations, including toxicity, resistance, and interactions with other commonly prescribed drugs. This has led to increasing interest in studying mechanisms underlying resistance and virulence of *Candida* species with the ultimate goal to identify potential drug targets for novel antifungal therapeutic intervention. However, the diploid nature and the absence of a complete sexual cycle in most *Candida* species limit the use of classical genetic approaches to dissect mechanisms controlling fungal fitness and antifungal resistance. Alternatively, applying genome-wide transcriptional methods such as those determining gene expression changes (DNA microarrays and transcriptome sequencing [RNA-seq]) or genomic occupancy (chromatin immunoprecipitation with microarray technology [ChIP-chip] and chromatin immunoprecipitation-DNA sequencing [ChIP-seq]) in *Candida* species had significantly contributed to uncovering different facets of fungal biology that are critical for both opportunistic and commensal lifestyles, in addition to antifungal tolerance and resistance (5–17). These approaches had also helped to uncover a surprising extent of evolutionary plasticity of transcriptional regulatory circuits in these species compared to the model yeast *Saccharomyces cerevisiae* (18, 19).

While ChIP-chip and ChIP-seq have been traditionally used to unbiasedly map the binding of a transcriptional regulator (TR), this tool has some limitations that are attributed mainly to TR-DNA cross-linking and DNA shearing by sonication (20). Formaldehyde is commonly used for protein-DNA cross-linking; however, this chemical preferentially generates protein-protein cross-links which can cause epitope masking and consequently alters the efficiency of the immunoprecipitation procedure and leads to increased signal background noise. Furthermore, DNA fragmentation by sonication can disrupt weak or transient TR-DNA or TR-histone interactions and generate DNA fragments with heterogenous sizes and thus impede the refinement of binding site identification (21).

To circumvent these limitations, cross-linking- and sonication-free alternative methods have been developed recently (20, 22–25). In one such method termed chromatin endogenous cleavage (ChEC) (26), the TR of interest is fused to the micrococcal nuclease (MNase) in order to fragment unprotected neighboring chromatin upon MNase activation by calcium (26). ChEC coupled to high-throughput sequencing (ChEC-seq) was efficiently used to map the binding of the general transcription factors Reb1, Abf1, and Rap1 in the budding yeast and has provided a high-resolution occupancy with more binding events than ChIP-based tools (20). Additionally, temporal analysis of ChEC-seq data uncovered that TR can have two distinct binding behaviors: a fast binding uncovered by rapid MNase cleavage at a locus with a robust bona fide TR-binding motif and a second slow cleavage with low-scoring motifs that are preferentially sampled by a given TR. ChEC-seq has been successfully used to define genomic occupancy of the chromatin remodeler RSC complex (Rsc8 subunit) as the ChIP procedure was less efficient (27, 28). Several recent investigations took advantage of ChEC-seq to study the role of different core components of the general transcriptional machinery such as mediators, SAGA (Spt-Ada-Gcn5-acetyltransferase), histone acetyltransferases, and chromatin "pushers," on global gene expression control and promoter nucleosome architecture in eukaryotes (29–32).

In this work, we describe a new set of PCR-based MNase-tagging plasmids for *C. albicans* and other *Candida* species to determine genome-wide location of any TR of interest by ChEC-seq. In a proof-of-concept application of ChEC-seq in *C. albicans*, we have selected Nsi1 that is an ortholog of the DNA-binding protein Reb1 for which

genome-wide occupancy was previously established by ChEC-seq in *S. cerevisiae* (20). As our previous effort on mapping occupancy of the *C. albicans* chromatin remodeling complex SWI/SNF by ChIP-tiling arrays had led to substantial background noise (7), we have used the ChEC-seq assay to obtain a high-resolution binding map of this master regulator of fungal fitness (6). The ChEC-seq procedure described here will allow a high-resolution genomic location definition which will enable a better understanding of transcriptional regulatory circuits that govern fungal fitness and drug resistance in these medically important fungi.

## RESULTS AND DISCUSSION

**Plasmid toolbox for MNase tagging in *C. albicans* and non-*albicans Candida* species.** We have previously constructed a series of pFA plasmids for C-terminal hemagglutinin (HA), tandem affinity purification (TAP), and MYC tagging in *C. albicans* with the *URA3*, *HIS1*, and *ARG4* autotrophy markers (33). Here, we have used these plasmids as a starting point to build new pFA plasmids that allow C-terminal tagging of any protein of interest at its native chromosomal location with the MNase. We synthesized a DNA construct encoding a 3xFLAG epitope and MNase that have been codon optimized for *C. albicans*. This construct was used to replace the DNA sequence of the TAP tag in pFA-TAP-CaURA3, pFA-TAP-CaHIS1, and pFA-TAP-CaARG4 to generate pFA-MNase-CaURA3, pFA-MNase-CaHIS1, and pFA-MNase-CaARG4, respectively. These plasmids allow the use of a single 120-bp primer pair (20 bp of vector sequences and 100 bp from the gene to be tagged) for PCR-based tagging of endogenous loci in *C. albicans* (Fig. 1A). These primers are compatible with the pFA-TAP/HA/MYC (33) and the pFA-XFP tagging systems (34, 35). We have also constructed the pFA-MNase-SAT1 plasmid with the dominant selectable marker *SAT1* that confers resistance to the antibiotic nourseothricin for MNase tagging in clinical strains of *C. albicans* and non-*albicans Candida* species such as the superbug *C. auris*.

**ChEC-seq experimental procedure.** ChEC-seq was initially used in *S. cerevisiae* to map the genomic occupancy of canonical general regulatory factors such as the RNA polymerase I enhancer-binding protein Reb1 (ScReb1) (20). Here, we have selected Nsi1 (C6_03550C_A), which is the ScReb1 ortholog in *C. albicans*, to perform ChEC-seq. Additionally, we were also interested in the catalytic subunit of the SWI/SNF complex, Snf2, to explore the potential of ChEC-seq in mapping genomic occupancy of chromatin remodeling complexes. We have previously mapped the genomic location of *C. albicans* Snf6, which is a fungus-specific SWI/SNF subunit, using ChIP coupled to high-density tiling arrays (7). Thus, the SWI/SNF genome-wide binding data generated by ChEC-seq can be compared to the benchmark data sets generated by ChIP-chip. We also generated an MNase control strain ("free MNase") with a 3xFLAG-tagged MNase module fused to a simian virus 40 (SV40) nuclear localization signal under the control of *ACT1* and integrated at the *RPS1* locus. Constitutive expression of MNase (free MNase) or MNase tagging of Nsi1 or Snf2 had no perceptible effect on the growth of *C. albicans* at different temperatures and stress conditions (Fig. 1B; see also Fig. S1 in the supplemental material).

The Nsi1 ortholog of *C. auris* was also MNase tagged using PCR cassettes generated from the pFA-MNase-SAT1 plasmid. For the MNase control strain, a 3xFLAG-tagged MNase module was inserted into the neutral intergenic locus *CauNI* where integration has no effect on the *in vitro* fitness of *C. auris* (Fig. 1B). As for *C. albicans*, MNase tagging of CauNsi1 does not affect the growth of *C. auris* (Fig. 1B and Fig. S1).

The *S. cerevisiae* ChEC procedure described by Zentner et al. (20) was followed with some modifications (Fig. 1C). *C. albicans* cells were permeabilized with digitonin for 10 min prior to MNase activation with 5 mM $CaCl_2$. We assumed that treating permeabilized cells with calcium would engender both specific and nonspecific cleavages. We therefore made a size selection of the ChEC DNA before preparing the sequencing library to enrich small fragments less than 400 bp. Prior to size selection and for each transcriptional regulator and the free MNase strain, we analyzed the kinetics of DNA digestion by agarose gel electrophoresis. Analysis of minute-scale time points revealed

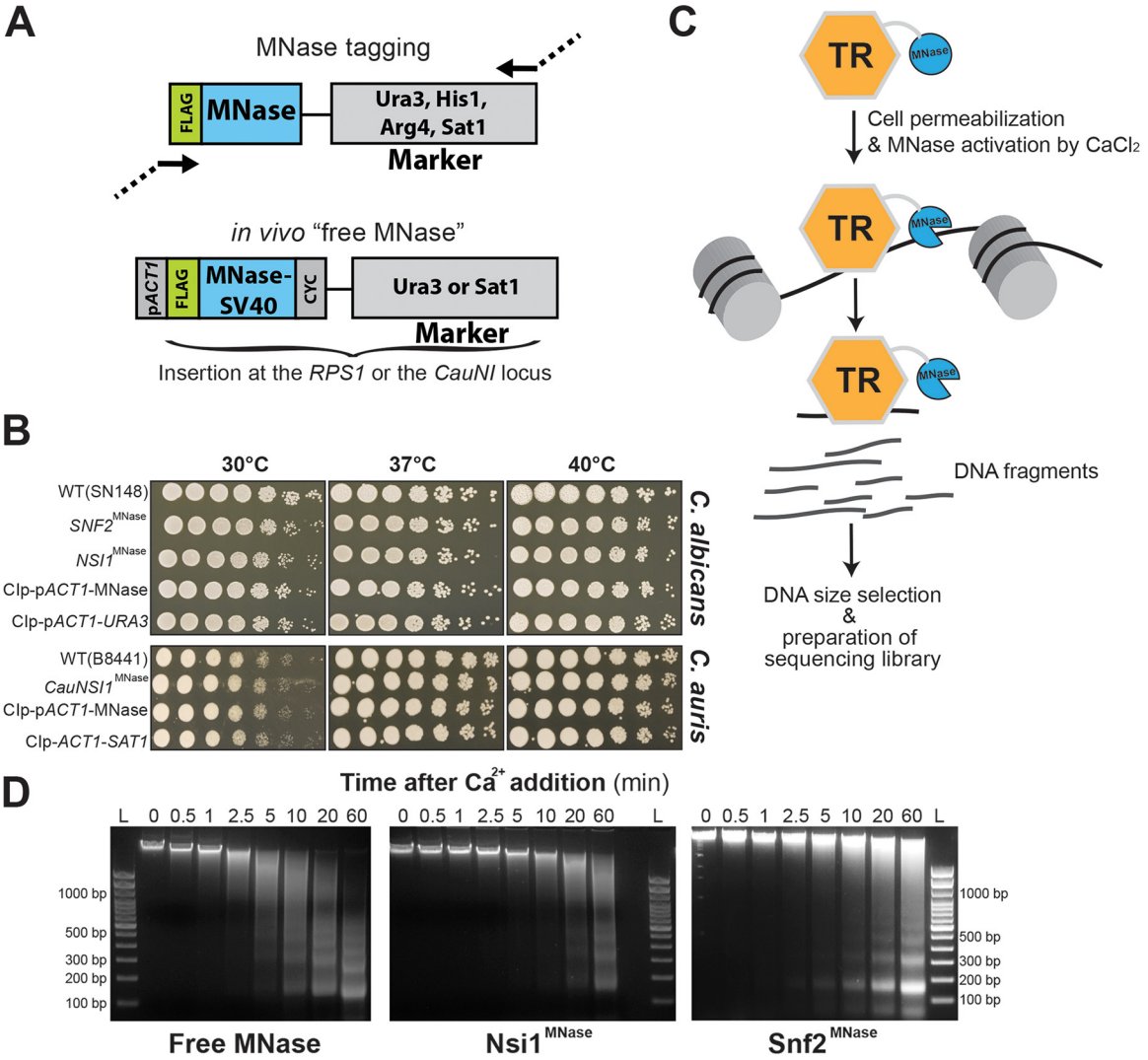


**FIG 1** ChEC-seq method in *C. albicans* and *Candida* spp. (A) Plasmid constructs for *in vivo* TR-MNase tagging and the construction of the "free MNase" control strains in *C. albicans* and *C. auris*. Structure of the MNase-tagging cassette consisting of a 3xFLAG epitope fused to the *C. albicans* codon-optimized MNase. The FLAG-MNase construct for the "free MNase" strain was constitutively expressed using the *C. albicans ACT1* promoter (p*ACT1*). CYC, *CYC1* terminator; SV40, nuclear localization signal. (B) Phenotypic characterization of strains bearing the MNase-tagged Nsi1 and Snf2 TRs and the "free MNase" control constructs in *C. albicans*. WT, Snf2$^{MNase}$, Nsi1$^{MNase}$, the free MNase, and the control (empty vector) strains were serially diluted, spotted on YPD, and incubated for 1 day at different temperatures. Growth patterns at different temperatures of the *C. auris* WT, CauNsi1$^{MNase}$, the free MNase and the control strains are also shown. (C) Schematic representation of the experimental setup of the ChEC-seq methodology. *Candida* species cells where a TR of interest is fused to MNase are permeabilized with digitonin prior to MNase activation with calcium. This will lead to the fragmentation of unprotected neighboring chromatin. The resulting fragmented DNA is purified and subjected to size selection prior to high-throughput sequencing. (D) Evaluation of genomic DNA fragmentation by agarose gel electrophoresis at 0, 0.5, 1, 2.5, 5, 10, 20, and 60 min of calcium exposure in the Snf2$^{MNase}$, Nsi1$^{MNase}$, and the free MNase strains in *C. albicans*. L, 100-bp DNA ladder.

notable smearing of genomic DNA of all TF-MNase fusions by the 5-min time point. This pattern increased over time until 60 min. In contrast, digestion in the free MNase strain yield smearing as early as 30 s (Fig. 1D). The 5-, 20-, and 60-min digestion times were selected for both Snf2 and Nsi1 ChEC-seq experiments. Size selection was performed using the Pippin Prep size selection system with 2% agarose gel cassette. The goal of this stage is to remove multikilobase fragments of genomic DNA and enrich small fragments. The 2% agarose gel cassette allows enrichment of DNA fragments below 100 to 400 bp. Alternatively, size selection could be performed using the paramagnetic beads and buffer exchange steps such as the AMPure XP cleanup kit (Beckman coulter) (20, 36). For *C. auris*, similar cell permeabilization and MNase activation procedures were

followed. The DNA digestion pattern showed a clear smearing at 20 min and 10 min for the "free MNase" and the CauNsi1-MNase strains, respectively (Fig. S2).

**Genome-wide binding of Nsi1 and Snf2 by ChEC-seq.** To provide a proof of principle for using ChEC in *Candida* spp., we focused our effort on *C. albicans*. To assess the ChEC-seq performance in *C. albicans*, we have chosen to map the genomic occupancy of Nsi1, which is an ortholog of the DNA-binding protein Reb1 for which the genome-wide occupancy was previously established by ChEC-seq in *S. cerevisiae* (20). We detected 2,548, 4,771, and 4,523 Nsi1 peaks upon 5, 20, and 60 min MNase activation, respectively (see Table S2 in the supplemental material and Fig. 2A). *De novo* motif analysis of intergenic bound Nsi1 regions showed a significant enrichment of the bona fide Reb1/Nsi1 site (TTACCCGG) at 5 min, while a nonspecific long AC/TG-rich sequence was the most enriched at 20 and 60 min (Fig. 2B). This suggests that the 5 min MNase cleavage mapped the Nsi1 fast class binding events, while 20 and 60 min captured the slow class binding that lacks the robust consensus motif. Thus, as for *S. cerevisiae*, our ChEC-seq data recapitulated the time-dependent binding behavior of transcriptional regulators and can be used to map early high-affinity interactions with consensus motifs and sequence that are preferentially sampled by a given protein (20). While the fast high-scoring sites are robust binding events, the slow low-scoring sites should be interpreted with caution since they might recapitulate nonspecific MNase cleavages that are near high-scoring sites in accessible chromatin (37, 38). For instance, and to identify high-confidence slow sites, slow ChEC-seq binding events should be matched with the set of transcripts with altered levels in a TR mutant to assess whether TR occupancy correlates with gene expression alterations at bound loci. Our genome-wide occupancy data recapitulated the overall functions of either Nsi1 or Reb1 in *S. cerevisiae* as reflected by Nsi1 binding to the promoter of ribosome biogenesis and rRNA genes (Fig. 2C to F) (39–41).

ChEC-seq of Snf2 identified 4,145, 6,446, and 6,215 peaks at 5, 20, and 60 min MNase cleavage, respectively, which is 10-fold higher than the number of peaks detected under similar growth conditions by ChIP-tiling array of the SWI/SNF subunit, Snf6 (7) (Fig. 3A and B and Table S3). As for Nsi1, the 20 and 60 min ChEC-seq data were similar and might capture the slow sites. The Snf2 fast bound promoters were enriched mainly in carbohydrate metabolism mirroring the previously characterized role of the SWI/SNF complex in *C. albicans* (Fig. 3C) (6, 7). Snf2 occupied promoters of hexose transport and carbon utilization genes (galactolysis) that were previously shown to be modulated by the SWI/SNF subunit Snf5 (6) (Fig. 3D).

**Conclusion.** We have constructed a new set of PCR-based MNase-tagging plasmids to map genomic occupancy of different transcriptional regulators in the human-pathogenic yeast *C. albicans* and other non-*albicans Candida* species. Compared to the other ChIP-based techniques, the ChEC procedure relies on total DNA extraction instead of chromatin solubilization and does not require protein-DNA cross-linking or sonication, thus avoiding artifacts related to epitope masking or the hyper-ChIPable euchromatic phenomenon (42, 43). So far, ChEC has been exclusively used in the model yeast *S. cerevisiae* to map chromatin occupancy of general transcriptional regulators (44), chromatin remodelers (27, 30, 45), and histone modifiers (31, 32) in addition to transcription factors (46, 47). As many transcriptional regulators and chromatin remodelers are key virulence and drug resistance factors in *C. albicans* and other fungi (6, 13, 17, 48–50), ChEC-seq represents an attracting tool to unbiasedly decipher transcriptional regulatory networks of fungal fitness.

## MATERIALS AND METHODS

**Strains, media, and growth assays.** *C. albicans* was routinely maintained at 30°C on YPD (1% yeast extract, 2% peptone, and 2% dextrose with 50 mg/ml uridine). The *C. albicans* wild-type (WT) strain SN148 (*his1/his1 leu2/leu2 arg4/arg4 ura3/ura3::imm434 IRO1/iro1::imm434*) (51) used in this study derives from the SC5314 clinical strain. For *C. auris*, the clinical B8441 strain (52) was used for *SAT1*-MNase tagging. For spot dilution assays, overnight cultures of both *C. albicans* and *C. auris* were diluted to an optical density at 600 nm ($OD_{600}$) of 1 and 5-fold serial dilutions were prepared in distilled water. A total of 4 $\mu$l of each dilution was spotted on YPD agar plates for 1 day at different temperatures (30°C, 37°C,

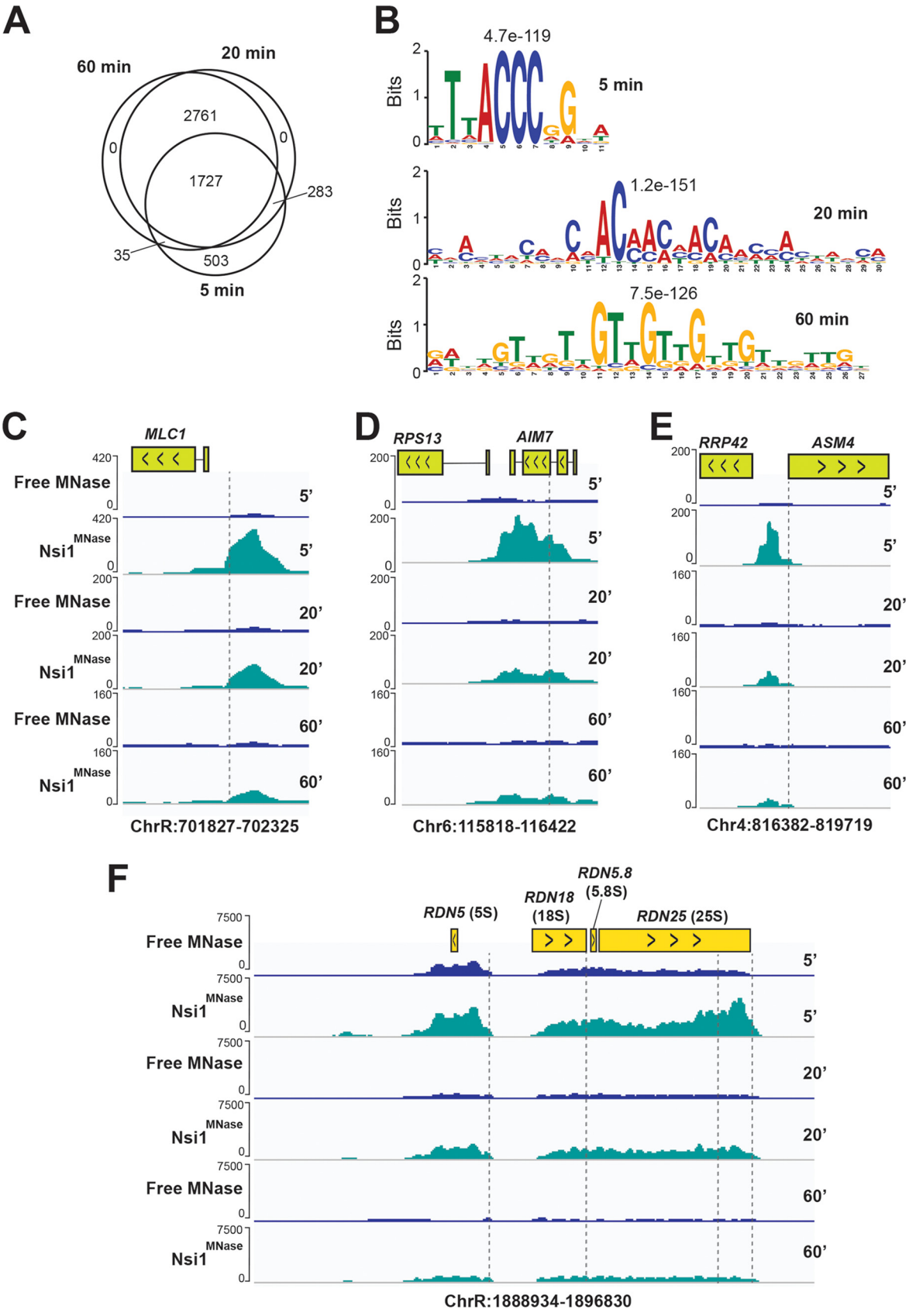


**FIG 2** Genome-wide occupancy of the transcription factor Nsi1 with ChEC-seq. (A) Temporal analysis of Nsi1 binding events. Venn diagram showing the overlap of Nsi1 binding events at three distinct MNase activation times (5, 20, and 60 min). (B) Motif scores for Nsi1-bound

(Continued on next page)

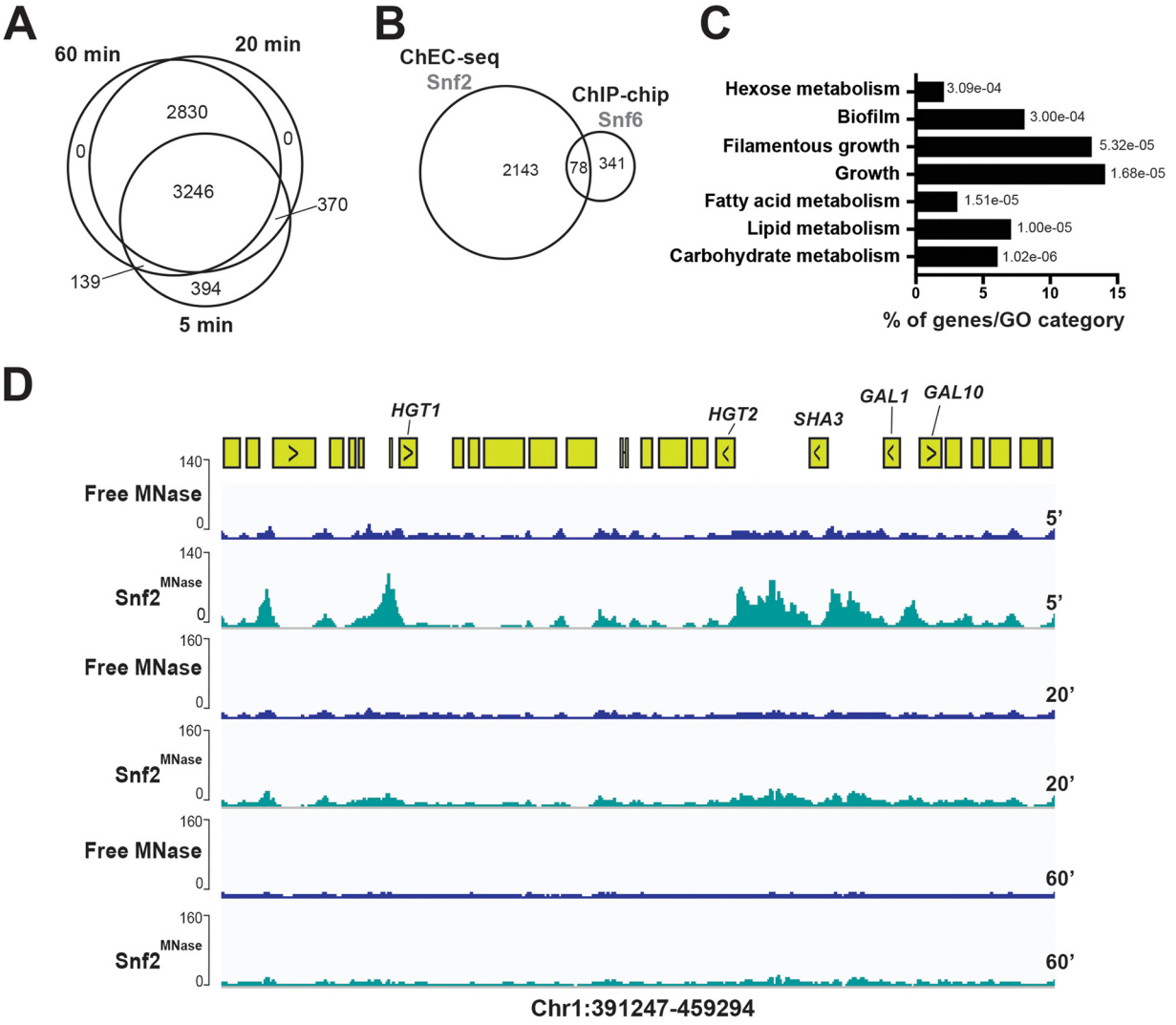


**FIG 3** Genome-wide occupancy of the chromatin remodeler Snf2 with ChEC-seq. (A) Venn diagram showing the overlap of Snf2 promoter binding at 5, 20, and 60 min after MNase activation. (B) Comparison of SWI/SNF genomic occupancies by ChEC-seq and ChIP-chip method. Venn diagram of overlap between Snf2 ChEC-seq sites and Snf6 ChIP-chip using high-density tiling arrays. (C) Gene ontology of biological process associated with Snf2-bound promoters at 5 min after MNase activation. The *P* values were calculated using hypergeometric distribution as described in the GO Term Finder Tool website (http://candidagenome.org/cgi-bin/GO/goTermFinder). (D) Snapshot of genomic regions showing the ChEC-seq signal for Snf2$^{MNase}$ and the free MNase strains at 5, 20, and 60 min after MNase activation. Genome browser view of Snf2 ChEC-seq displaying promoter occupancies of carbohydrate metabolism genes, including galactolysis (*GAL1* and *GAL10*) and hexose transport (*SHA3*, *HGT2*, and *HGT1*).

and 40°C) and imaged using the SP imager system. For growth assays in liquid media, overnight cultures of *C. albicans* and *C. auris* were resuspended in fresh YPD medium at an $OD_{600}$ of 0.05 and added to a flat-bottom 96-well plate in a total volume of 100 $\mu$l per well in addition to the tested compounds (fluconazole [1 $\mu$g/ml] and sodium chloride [0.3 M]). Growth of the MNase-tagged and the control strains was also assessed in the synthetic complete (SC) medium. For each experiment, a compound-free and a cell-free negative control were included. Growth assay curves were performed in triplicate in 96-well plates using a Sunrise plate reader (Tecan) at 30°C with constant agitation with $OD_{600}$ readings taken at 24 h. The relative growth was determined as the OD ratio of the YPD control to the treated cultures and is expressed as a percentage. The results are the means of the results from at least three biological replicates. Statistical significance was tested using Student's *t* test.

**FIG 2** Legend (Continued)
promoters at 5, 20, and 60 min after MNase activation. The motif logos were generated using MEME-ChIP software on the 1,000 high-scoring peaks. (C to F) Snapshots of genomic regions showing the ChEC-seq signal for Nsi1$^{MNase}$ and the free MNase strains at 5, 20, and 60 min after MNase activation. The positions of the Nsi1 motifs are indicated by the dashed lines. Nsi1 occupies the promoter of *MLC1* (C), *AIM7* (D), and *ASM4* (E), in addition to many sites within the rDNA locus (F).

**Construction of the pFA-MNase plasmids and the "free MNase" control strains.** The pFA-MNase-CaURA3, pFA-MNase-CaHIS1, and pFA-MNase-CaARG4 plasmids were constructed as follows. DNA of the 3xFLAG epitope-MNase module was synthesized by Biobasic, codon optimized for *C. albicans* (a total of 11 CTG codons of the MNase were changed to TTA or TTG). The PacI-AscI 3xFLAG-MNase fragment was cloned in the PacI-AscI-digested pFA-TAP-CaURA3, pFA-TAP-CaHIS1, and pFA-TAP-CaARG4 (33). For pFA-MNase-*SAT1*, pFA-MNase-Ca*URA3* was double digested with AscI and SacI restriction enzymes to remove the *URA3* auxotrophy marker. The *SAT1* marker was amplified from pFA-SAT1 (34) with primers (see Table S1 in the supplemental material) containing restriction sites AscI-SacI and cloned into the AscI-SacI-digested pFA-MNase. The resulting pFA-MNase-SAT1 was sequenced to confirm the integrity of the Sat1 dominant marker.

The free MNase control strain was constructed as follows. The *C. albicans* codon-optimized DNA of the 3xFLAG-MNase-nuclear localization signal (SV40) (3xFLAG-MNase-SV40) construct delimited by NheI and MluI restriction sites was synthesized. The NheI-MluI-digested 3xFLAG-MNase-SV40 fragment was then cloned into the CIp-p*ACT1*-CYC vector (53) to ensure constitutive expression of MNase in *C. albicans*. The CIp-p*ACT1*-3xFLAG-MNase-SV40-CYC plasmid was linearized by StuI restriction enzyme and integrated at the *RPS1* locus of the SN148 WT strain.

For the *C. auris* MNase control strain, the *URA3* auxotrophy marker of the CIp-p*ACT1*-3xFLAG-MNase-SV40-CYC was replaced by SAT1 as follows. The *SAT1* marker was amplified from pFA-SAT1 with primers containing restriction sites NotI-NheI (Table S1) and cloned into the NotI-NheI-digested CIp-p*ACT1*-3xFLAG-MNase-SV40-CYC. To allow the integration of the CIp-p*ACT1*-3xFLAG-MNase-SV40-CYC in the *C. auris* genome, the *C. albicans RPS1* integrative locus was replaced by a short 900-bp *C. auris* intergenic region *CauNI* (*C. auris* neutral intergenic; GenBank accession no. PEKT02000001: 871,442 to 872,342) as follows. The *CauNI* region was amplified from the *C. auris* B8441 genomic DNA with primers containing restriction sites SacII-NotI (Table S1) and cloned into the SacII-NotI-digested CIp-p*ACT1*-3xFLAG-MNase-SV40-CYC-*SAT1* plasmid. The resulting plasmid was linearized by SacII restriction enzyme and integrated at the *CauNI* locus of the *C. auris* B8441 strain. The correct integration of the CIp-p*ACT1*-3xFLAG-MNase-SV40-CYC-*SAT1* cassette was verified by PCR. Integration of any exogenous DNA or the CIp-p*ACT1*-3xFLAG-MNase-SV40-CYC-*SAT1* at the *CauNI* has no impact on the *in vitro* growth of *C. auris*.

**PCR-based tagging of endogenous loci in *C. albicans* and *C. auris*.** *SNF2* (C2_02100W_A) and *NSI1* (C6_03550C_A) were MNase tagged *in vivo* with the MNase cassette PCR products following the protocol described by Lavoie et al. (33). The MNase cassettes were amplified using a 120-bp primer pair with 20 bp of vector sequences (forward [GGTCGACGGATCCCCGGGTT] and reverse [TCGATGAATTCGAGCTCGTT]) and 100 bp from *SNF2* (C2_02100W_A) and *NSI1* (C6_03550C_A) (Table S1). PCRs were performed in 50-$\mu$l volumes with 1 ng pFA-MNase plasmid and the Q5 high-fidelity polymerase (New England Biolabs). PCR thermocycling was executed as follows: (i) initial denaturing, 98°C for 30 s; (ii) 10 cycles with 1 cycle consisting of 98°C for 10 s, 50°C for 1 min, and 72°C for 3 min; and (iii) 25 cycles with 1 cycle consisting of 98°C for 30 s, 55°C for 1 min, and 72°C for 3 min. PCR products were used directly to transform the WT strain SN148 using a lithium acetate transformation protocol (54). Transformants were selected on selective plates, and positive colonies were analyzed by PCR to confirm the correct integration of the MNase tag. For *C. auris*, *CauNSI1* (B9J08_003000) was MNase tagged *in vivo* with the MNase-*SAT1* cassette as described for *C. albicans* with the exception that a reverse vector sequence of 24 bp was used (TCTGATATCATCGATGAATTCGAG).

**ChEC-seq procedure.** For each ChEC experiment, saturated overnight cultures of *C. albicans* MNase tagged and free MNase strains were diluted to a starting $OD_{600}$ of 0.1 in 50 ml YPD medium and grown at 30°C to an $OD_{600}$ of 0.7 to 0.8. Cells were pelleted at 3,000 $\times$ *g* for 5 min and washed three times with 1 ml buffer A (15 mM Tris [pH 7.5], 80 mM KCl, 0.1 mM EGTA, 0.2 mM spermine, 0.5 mM spermidine, one tablet Roche cOmplete EDTA-free mini protease inhibitors, 1 mM phenylmethylsulfonyl fluoride [PMSF]). Cells were then resuspended in 800 $\mu$l buffer A containing 0.1% digitonin (Sigma) and permeabilized for 10 min at 30°C with shaking. MNase digestions were performed by adding $CaCl_2$ to a final concentration of 5 mM and incubated for the indicated time at 30°C. At each time point, a total of 200-$\mu$l aliquots of the ChEC digestions were transferred to a tube containing 50 $\mu$l of 250 mM EGTA to quench MNase digestion. For each factor analyzed, the time point zero corresponds to a condition where MNase was not activated by $CaCl_2$. Nucleic acids were extracted using MasterPure yeast DNA purification kit (Epicentre, MPY80200) according to the manufacturer's instructions and resuspended in 50 $\mu$l of 10 mM Tris-HCl buffer, pH 8.0. RNAs were digested with 10 $\mu$g RNase A at 37°C for 20 min. To assess MNase activity, 5 $\mu$l of digested DNA of each ChEC time point (time after $CaCl_2$ addition) was loaded on a 1.5% agarose gel. ChEC DNA was subjected to size selection using the Pippin Prep (SageScience) size selection system with a 2% agarose gel cassette, allowing the removal of multikilobase genomic DNA fragments and the enrichment of 100- to 400-bp DNA fragments. For *C. auris*, the ChEC procedure was the same as for *C. albicans* except that MNase activation was performed at 37°C.

**Library preparation, next-generation sequencing (NGS), and peak calling.** The NEBNext Ultra II DNA Library Prep kit for Illumina was used to construct the ChEC-seq library following the manufacturer's instruction. The quality, quantity, and size distribution of the libraries were determined using an Agilent bioanalyzer. A 50-bp single-end sequencing of DNAs was performed using an Illumina HiSeq 4000 sequencing system. Sequences were trimmed to remove adapters using TRIMMOMATIC with options "TRAILING:30" (55). Reads thus obtained were mapped to the *C. albicans* genome (*Candida_albicans*_SC5314 assembly 22) (56) using Bowtie2 with "-q --phred33 --no-unal" options (57). Peaks were determined using MACS2 algorithm (58) with options "-BAM -nomodel-extsize 200-keep-dup all." MACS2 outputs BED6+4 format files that contain the peak locations (narrowPeak) and peak summit locations for each peak. The biological replicates were merged into single samples, retaining all high-confidence peaks

(q-value cutoff = 0.05) from all replicates. Read alignment, peaks, and track visualization using bedgraph files were performed as previously described (20, 44). BigWig files were also generated to visualize the different ChEC-seq tracks on the Integrative Genomics Viewer (IGV) (https://igv.org) interface. *cis*-Regulatory motif enrichment was assessed in the top high-scoring 1,000 peaks for both Nsi1 and Snf2 using MEME-ChIP software (59).

**Data availability.** The sequences of plasmids pFA-MNase-CaHIS1, pFA-MNase-CaARG4, pFA-MNase-CaURA3, and pFA-MNase-SAT1 have been submitted to GenBank and have been assigned the following accession numbers: MT181237, MT181238, MT181239, and MT223485. All ChEC-seq data generated in this study were submitted to GEO database under the accession number GSE150063.

## SUPPLEMENTAL MATERIAL

Supplemental material is available online only.

**FIG S1**, TIF file, 0.5 MB.

**FIG S2**, TIF file, 0.3 MB.

**TABLE S1**, XLSX file, 0.02 MB.

**TABLE S2**, XLSX file, 0.3 MB.

**TABLE S3**, XLSX file, 0.4 MB.

## ACKNOWLEDGMENTS

We thank Benjamin Albert and David Shore (University of Geneva) for sharing reagents and their technical guidance regarding the ChEC protocol. We thank Senthil Kumar Duraikannu Kailasam (Canadian Centre for Computational Genomics, McGill University) for his valuable assistance with the ChEC-seq data processing and analysis.

This work was supported by funds from the Canadian Institutes for Health Research (CIHR) project grant (grant IC118460) and the start-up funds from the Montréal Heart Institute (MHI) to A.S. A.S. is a recipient of the Fonds de Recherche du Québec-Santé (FRQS) J2 salary award.

## REFERENCES

1. Sabino R, Veríssimo C, Pereira ÁA, Antunes F. 2020. Candida auris, an agent of hospital-associated outbreaks: which challenging issues do we need to have in mind? Microorganisms 8:181. https://doi.org/10.3390/microorganisms8020181.
2. Dufresne SF, Cole DC, Denning DW, Sheppard DC. 2017. Serious fungal infections in Canada. Eur J Clin Microbiol Infect Dis 36:987–992. https://doi.org/10.1007/s10096-017-2922-y.
3. Gabaldón T, Naranjo-Ortíz MA, Marcet-Houben M. 2016. Evolutionary genomics of yeast pathogens in the Saccharomycotina. FEMS Yeast Res 16:fow064. https://doi.org/10.1093/femsyr/fow064.
4. Turner SA, Butler G. 2014. The Candida pathogenic species complex. Cold Spring Harb Perspect Med 4:a019778. https://doi.org/10.1101/cshperspect.a019778.
5. Chen C, Pande K, French SD, Tuch BB, Noble SM. 2011. An iron homeostasis regulatory circuit with reciprocal roles in Candida albicans commensalism and pathogenesis. Cell Host Microbe 10:118–135. https://doi.org/10.1016/j.chom.2011.07.005.
6. Burgain A, Pic É, Markey L, Tebbji F, Kumamoto CA, Sellam A. 2019. A novel genetic circuitry governing hypoxic metabolic flexibility, commensalism and virulence in the fungal pathogen Candida albicans. PLoS Pathog 15:e1007823. https://doi.org/10.1371/journal.ppat.1007823.
7. Tebbji F, Chen Y, Sellam A, Whiteway M. 2017. The genomic landscape of the fungus-specific SWI/SNF complex subunit, Snf6, in Candida albicans. mSphere 2:e00497-17. https://doi.org/10.1128/mSphere.00497-17.
8. Askew C, Sellam A, Epp E, Hogues H, Mullick A, Nantel A, Whiteway M. 2009. Transcriptional regulation of carbohydrate metabolism in the human pathogen Candida albicans. PLoS Pathog 5:e1000612. https://doi.org/10.1371/journal.ppat.1000612.
9. Perez JC, Kumamoto CA, Johnson AD. 2013. Candida albicans commensalism and pathogenicity are intertwined traits directed by a tightly knit transcriptional regulatory circuit. PLoS Biol 11:e1001510. https://doi.org/10.1371/journal.pbio.1001510.
10. Nobile CJ, Fox EP, Nett JE, Sorrells TR, Mitrovich QM, Hernday AD, Tuch BB, Andes DR, Johnson AD. 2012. A recently evolved transcriptional network controls biofilm development in Candida albicans. Cell 148:126–138. https://doi.org/10.1016/j.cell.2011.10.048.
11. Nobile CJ, Nett JE, Hernday AD, Homann OR, Deneault J-S, Nantel A, Andes DR, Johnson AD, Mitchell AP. 2009. Biofilm matrix regulation by Candida albicans Zap1. PLoS Biol 7:e1000133. https://doi.org/10.1371/journal.pbio.1000133.
12. Tierney L, Linde J, Müller S, Brunke S, Molina J, Hube B, Schöck U, Guthke R, Kuchler K. 2012. An interspecies regulatory network inferred from simultaneous RNA-seq of Candida albicans invading innate immune cells. Front Microbiol 3:85. https://doi.org/10.3389/fmicb.2012.00085.
13. Price RJ, Weindling E, Berman J, Buscaino A. 2019. Chromatin profiling of the repetitive and nonrepetitive genomes of the human fungal pathogen *Candida albicans*. mBio 10:e01376-19. https://doi.org/10.1128/mBio.01376-19.
14. Tucey TM, Verma J, Harrison PF, Snelgrove SL, Lo TL, Scherer AK, Barugahare AA, Powell DR, Wheeler RT, Hickey MJ, Beilharz TH, Naderer T, Traven A. 2018. Glucose homeostasis is important for immune cell viability during Candida challenge and host survival of systemic fungal infection. Cell Metab 27:988–1006.e7. https://doi.org/10.1016/j.cmet.2018.03.019.
15. Liu TT, Znaidi S, Barker KS, Xu L, Homayouni R, Saidane S, Morschhauser J, Nantel A, Raymond M, Rogers PD. 2007. Genome-wide expression and location analyses of the Candida albicans Tac1p regulon. Eukaryot Cell 6:2122–2138. https://doi.org/10.1128/EC.00327-07.
16. Shapiro RS, Robbins N, Cowen LE. 2011. Regulatory circuitry governing fungal development, drug resistance, and disease. Microbiol Mol Biol Rev 75:213–267. https://doi.org/10.1128/MMBR.00045-10.
17. Villa S, Hamideh M, Weinstock A, Qasim MN, Hazbun TR, Sellam A, Hernday AD, Thangamani S. 2020. Transcriptional control of hyphal morphogenesis in Candida albicans. FEMS Yeast Res 20:foaa005. https://doi.org/10.1093/femsyr/foaa005.
18. Lavoie H, Hogues H, Whiteway M. 2009. Rearrangements of the transcriptional regulatory networks of metabolic pathways in fungi. Curr Opin Microbiol 12:655–663. https://doi.org/10.1016/j.mib.2009.09.015.
19. Li H, Johnson AD. 2010. Evolution of transcription networks–lessons from yeasts. Curr Biol 20:R746–R753. https://doi.org/10.1016/j.cub.2010.06.056.
20. Zentner GE, Kasinathan S, Xin B, Rohs R, Henikoff S. 2015. ChEC-seq kinetics discriminates transcription factor binding sites by DNA se-

quence and shape in vivo. Nat Commun 6:8733. https://doi.org/10.1038/ncomms9733.
21. Zentner GE, Henikoff S. 2014. High-resolution digital profiling of the epigenome. Nat Rev Genet 15:814–827. https://doi.org/10.1038/nrg3798.
22. van Steensel B, Henikoff S. 2000. Identification of in vivo DNA targets of chromatin proteins using tethered Dam methyltransferase. Nat Biotechnol 18:424–428. https://doi.org/10.1038/74487.
23. Wang H, Mayhew D, Chen X, Johnston M, Mitra RD. 2012. "Calling cards" for DNA-binding proteins in mammalian cells. Genetics 190:941–949. https://doi.org/10.1534/genetics.111.137315.
24. Kasinathan S, Orsi GA, Zentner GE, Ahmad K, Henikoff S. 2014. High-resolution mapping of transcription factor binding sites on native chromatin. Nat Methods 11:203–209. https://doi.org/10.1038/nmeth.2766.
25. Meers MP, Bryson TD, Henikoff JG, Henikoff S. 2019. Improved CUT&RUN chromatin profiling tools. Elife 8:e46314. https://doi.org/10.7554/eLife.46314.
26. Schmid M, Durussel T, Laemmli UK. 2004. ChIC and ChEC: genomic mapping of chromatin proteins. Mol Cell 16:147–157. https://doi.org/10.1016/j.molcel.2004.09.007.
27. Kubik S, O'Duibhir E, de Jonge WJ, Mattarocci S, Albert B, Falcone J-L, Bruzzone MJ, Holstege FCP, Shore D. 2018. Sequence-directed action of RSC remodeler and general regulatory factors modulates +1 nucleosome position to facilitate transcription. Mol Cell 71:89–102. https://doi.org/10.1016/j.molcel.2018.05.030.
28. Yen K, Vinayachandran V, Batta K, Koerber RT, Pugh BF. 2012. Genome-wide nucleosome specificity and directionality of chromatin remodelers. Cell 149:1461–1473. https://doi.org/10.1016/j.cell.2012.04.036.
29. Tourigny JP, Saleh MM, Schumacher K, Devys D, Zentner GE. 2018. Mediator is essential for small nuclear and nucleolar RNA transcription in yeast. Mol Cell Biol 38:e00296-18. https://doi.org/10.1128/MCB.00296-18.
30. Kubik S, Bruzzone MJ, Challal D, Dreos R, Mattarocci S, Bucher P, Libri D, Shore D. 2019. Opposing chromatin remodelers control transcription initiation frequency and start site selection. Nat Struct Mol Biol 26:744–754. https://doi.org/10.1038/s41594-019-0273-3.
31. Bruzzone MJ, Grünberg S, Kubik S, Zentner GE, Shore D. 2018. Distinct patterns of histone acetyltransferase and Mediator deployment at yeast protein-coding genes. Genes Dev 32:1252–1265. https://doi.org/10.1101/gad.312173.118.
32. Baptista T, Grünberg S, Minoungou N, Koster MJE, Timmers HTM, Hahn S, Devys D, Tora L. 2017. SAGA is a general cofactor for RNA polymerase II transcription. Mol Cell 68:130–143.e5. https://doi.org/10.1016/j.molcel.2017.08.016.
33. Lavoie H, Sellam A, Askew C, Nantel A, Whiteway M. 2008. A toolbox for epitope-tagging and genome-wide location analysis in Candida albicans. BMC Genomics 9:578. https://doi.org/10.1186/1471-2164-9-578.
34. Schaub Y, Dunkler A, Walther A, Wendland J. 2006. New pFA-cassettes for PCR-based gene manipulation in Candida albicans. J Basic Microbiol 46:416–429. https://doi.org/10.1002/jobm.200510133.
35. Gola S, Martin R, Walther A, Dunkler A, Wendland J. 2003. New modules for PCR-based gene targeting in Candida albicans: rapid and efficient gene targeting using 100 bp of flanking homology region. Yeast 20:1339–1347. https://doi.org/10.1002/yea.1044.
36. Grünberg S, Zentner GE. 2017. Genome-wide mapping of protein-DNA interactions with ChEC-seq in Saccharomyces cerevisiae. J Vis Exp 2017:55836. https://doi.org/10.3791/55836.
37. Rossi MJ, Lai WKM, Pugh BF. 2017. Correspondence: DNA shape is insufficient to explain binding. Nat Commun 8:15643. https://doi.org/10.1038/ncomms15643.
38. Kasinathan S, Zentner GE, Xin B, Rohs R, Henikoff S. 2017. Correspondence: Reply to 'DNA shape is insufficient to explain binding.' Nat Commun 8:15644. https://doi.org/10.1038/ncomms15644.
39. Bosio MC, Fermi B, Spagnoli G, Levati E, Rubbi L, Ferrari R, Pellegrini M, Dieci G. 2017. Abf1 and other general regulatory factors control ribosome biogenesis gene expression in budding yeast. Nucleic Acids Res 45:4493–4506. https://doi.org/10.1093/nar/gkx058.
40. Lang WH, Reeder RH. 1993. The REB1 site is an essential component of a terminator for RNA polymerase I in Saccharomyces cerevisiae. Mol Cell Biol 13:649–658. https://doi.org/10.1128/mcb.13.1.649.
41. Reiter A, Hamperl S, Seitz H, Merkl P, Perez-Fernandez J, Williams L, Gerber J, Németh A, Léger I, Gadal O, Milkereit P, Griesenbeck J, Tschochner H. 2012. The Reb1-homologue Ydr026c/Nsi1 is required for efficient RNA polymerase I termination in yeast. EMBO J 31:3480–3493. https://doi.org/10.1038/emboj.2012.185.
42. Teytelman L, Thurtle DM, Rine J, van Oudenaarden A. 2013. Highly expressed loci are vulnerable to misleading ChIP localization of multiple unrelated proteins. Proc Natl Acad Sci U S A 110:18602–18607. https://doi.org/10.1073/pnas.1316064110.
43. Park D, Lee Y, Bhupindersingh G, Iyer VR. 2013. Widespread misinterpretable ChIP-seq bias in yeast. PLoS One 8:e83506. https://doi.org/10.1371/journal.pone.0083506.
44. Grünberg S, Henikoff S, Hahn S, Zentner GE. 2016. Mediator binding to UASs is broadly uncoupled from transcription and cooperative with TFIID recruitment to promoters. EMBO J 35:2435–2446. https://doi.org/10.15252/embj.201695020.
45. Biernat E, Kinney J, Dunlap K, Rizza C, Govind CK. 2020. The RSC complex remodels nucleosomes in transcribed coding sequences and promotes transcription in Saccharomyces cerevisiae. bioRxiv https://doi.org/10.1101/2020.03.11.987974.
46. Albert B, Tomassetti S, Gloor Y, Dilg D, Mattarocci S, Kubik S, Hafner L, Shore D. 2019. Sfp1 regulates transcriptional networks driving cell growth and division through multiple promoter-binding modes. Genes Dev 33:288–293. https://doi.org/10.1101/gad.322040.118.
47. Bar-Ziv R, Brodsky S, Chapal M, Barkai N. 2020. Transcription factor binding to replicated DNA. Cell Rep 30:3989–3995.e4. https://doi.org/10.1016/j.celrep.2020.02.114.
48. Nishikawa JL, Boeszoermenyi A, Vale-Silva LA, Torelli R, Posteraro B, Sohn Y-J, Ji F, Gelev V, Sanglard D, Sanguinetti M, Sadreyev RI, Mukherjee G, Bhyravabhotla J, Buhrlage SJ, Gray NS, Wagner G, Näär AM, Arthanari H. 2016. Inhibiting fungal multidrug resistance by disrupting an activator–Mediator interaction. Nature 530:485–489. https://doi.org/10.1038/nature16963.
49. Kuchler K, Jenull S, Shivarathri R, Chauhan N. 2016. Fungal KATs/KDACs: a new highway to better antifungal drugs? PLoS Pathog 12:e1005938. https://doi.org/10.1371/journal.ppat.1005938.
50. Leach MD, Farrer RA, Tan K, Miao Z, Walker LA, Cuomo CA, Wheeler RT, Brown AJP, Wong KH, Cowen LE. 2016. Hsf1 and Hsp90 orchestrate temperature-dependent global transcriptional remodelling and chromatin architecture in Candida albicans. Nat Commun 7:11704. https://doi.org/10.1038/ncomms11704.
51. Noble SM, Johnson AD. 2005. Strains and strategies for large-scale gene deletion studies of the diploid human fungal pathogen Candida albicans. Eukaryot Cell 4:298–309. https://doi.org/10.1128/EC.4.2.298-309.2005.
52. Lockhart SR, Etienne KA, Vallabhaneni S, Farooqi J, Chowdhary A, Govender NP, Colombo AL, Calvo B, Cuomo CA, Desjardins CA, Berkow EL, Castanheira M, Magobo RE, Jabeen K, Asghar RJ, Meis JF, Jackson B, Chiller T, Litvintseva AP. 2017. Simultaneous emergence of multidrug-resistant Candida auris on 3 continents confirmed by whole-genome sequencing and epidemiological analyses. Clin Infect Dis 64:134–140. https://doi.org/10.1093/cid/ciw691.
53. Blackwell C, Russell CL, Argimon S, Brown AJ, Brown JD. 2003. Protein A-tagging for purification of native macromolecular complexes from Candida albicans. Yeast 20:1235–1241. https://doi.org/10.1002/yea.1036.
54. Hernday AD, Noble SM, Mitrovich QM, Johnson AD. 2010. Genetics and molecular biology in Candida albicans. Methods Enzymol 470:737–758. https://doi.org/10.1016/S0076-6879(10)70031-8.
55. Bolger AM, Lohse M, Usadel B. 2014. Trimmomatic: a flexible trimmer for Illumina sequence data. Bioinformatics 30:2114–2120. https://doi.org/10.1093/bioinformatics/btu170.
56. Skrzypek MS, Binkley J, Binkley G, Miyasato SR, Simison M, Sherlock G. 2017. The *Candida* Genome Database (CGD): incorporation of Assembly 22, systematic identifiers and visualization of high throughput sequencing data. Nucleic Acids Res 45:D592–D596. https://doi.org/10.1093/nar/gkw924.
57. Langmead B, Salzberg SL. 2012. Fast gapped-read alignment with Bowtie 2. Nat Methods 9:357–359. https://doi.org/10.1038/nmeth.1923.
58. Zhang Y, Liu T, Meyer CA, Eeckhoute J, Johnson DS, Bernstein BE, Nusbaum C, Myers RM, Brown M, Li W, Liu XS. 2008. Model-based analysis of ChIP-Seq (MACS). Genome Biol 9:R137. https://doi.org/10.1186/gb-2008-9-9-r137.
59. Machanick P, Bailey TL. 2011. MEME-ChIP: motif analysis of large DNA datasets. Bioinformatics 27:1696–1697. https://doi.org/10.1093/bioinformatics/btr189.